An Adaptive Feedback Canceller for Full-Duplex Relays Based on Spectrum Shaping

Roberto López-Valcarce, Emilio Antonio-Rodríguez, Carlos Mosquera and Fernando Pérez-González

***Abstract*—Although full-duplex relaying schemes are appealing in order to improve spectral efficiency, simultaneous reception and transmission in the same frequency results in self-interference, distorting the retransmitted signal and making the relay prone to oscillation. Current feedback cancellation techniques by means of adaptive filters are hampered by the fact that the useful and interference signals are highly correlated. We present a new adaptive algorithm which effectively and blindly restores the spectral shape of the desired signal. In contrast with previous schemes, the novel adaptive feedback canceller has low complexity, does not introduce additional delay in the relay station, and partly compensates for multipath propagation.**

***Index Terms*—Full-duplex, relays, adaptive algorithm, feedback cancellation.**

I. Introduction

The use of relays is a promising, cost-effective approach to extending wireless systems coverage [1], [2] and increasing the network throughput by providing cooperative diversity [3], [4]. Relay terminals can be either dedicated infrastructure-based transceivers, or mobile devices that forward signals from source to destination. To this day, most research has focused on *half-duplex* protocols, which constrain the relays to transmit and receive in different time slots and/or carrier frequencies. This facilitates relay design, since it avoids coupling between the transmit and receive frontends which would otherwise appear whenever these operate simultaneously within the same frequency channel. This coupling would result in self-interference, which is eliminated with the half-duplex approach at the cost of a reduction in spectral efficiency.

In contrast, *full-duplex* operation of a relay allows concurrent transmission and reception in a single time/frequency channel, thus improving spectral efficiency. Clearly, full-duplex relays must include mechanisms to mitigate self-interference. This is not a minor issue, given that the power of the signal that is transmitted by the relay may be tens of dB above that of the received signal. An exemplary application of full-duplex relays is found in the area of digital terrestrial broadcasting with single frequency networks (SFN), in order to improve reception in areas with poor coverage. In this context they are commonly referred to as *on-channel repeaters* and are being successfully deployed with SFN-based broadcast systems using Orthogonal Frequency Division Multiplexing (OFDM) [5], [6]. Full-duplex relaying is especially appealing for OFDM systems, since the signals originating from the source and the relay will add up at the destination as helpful multipath as long as their arrival times are within the cyclic prefix duration. This limits the processing delay allowable at the relay, which must be kept at a sufficiently low value.

Although on-channel repeaters incorporate physical separation of the transmit and receive antennas in order to reduce signal coupling and avoid system instability, this approach usually does not provide sufficient input/output isolation, even when antenna directivity is taken into account. In addition, local scatterers may create additional feedback paths between the antennas. Thus, adaptive feedback cancellation (AFC) via digital signal processing techniques has revealed itself as the key enabler for these devices, and will be necessary for the deployment of full-duplex relays in other types of networks as well [7]–[11]. The focus of this paper is the development of a novel AFC technique for full-duplex relays. The proposed method operates directly on waveform samples, and thus it is well suited for Amplify-and-Forward (A&F) relays. Although A&F relaying is not necessarily optimal, it is a highly flexible technology applicable even in heterogeneous networks with nodes having different characteristics, since it is transparent to the specific modulation type of the transmitted signal [12].

Direct application of the Least Mean Squares (LMS) adaptive algorithm [13], [14] to the AFC problem will result in significant bias in the estimation of the feedback path, since the signal arriving at the relay from the source is correlated with the feedback signal. Several works have addressed this bias problem in different ways. Introducing a sufficient amount of delay in the feedback loop of the AFC will decorrelate the received and feedback signals and hence eliminate the bias [5], [7], but this is at the expense of increasing the overall processing delay of the repeater, which is undesirable. Alternatively, in [15], [16] two whitening approaches are proposed in order to generate the signals that drive the AFC coefficient update; however, the length of the required whitening filter may add significant complexity to these schemes, especially for signals with low spectral flatness. Other approaches are based on introducing low-power training sequences at the relay [17],

R. López-Valcarce is with the Signal Theory and Communications Department, University of Vigo, Vigo, Spain (e-mail: valcarce@gts.uvigo.es).

E. Antonio-Rodríguez is with the Galician Research and Development Center in Advanced Telecommunications (GRADIANT), Vigo, Spain (e-mail: eantonio@gradiant.org).

C. Mosquera is with the Signal Theory and Communications Department, University of Vigo, Vigo, Spain, and also with GRADIANT (e-mail: mosquera@gts.uvigo.es).

F. Pérez-González is with the Signal Theory and Communications Department, University of Vigo, Vigo, Spain, with GRADIANT, and also with the Department of Electrical and Computer Engineering, University of New Mexico, Albuquerque, NM (e-mail: fperez@gts.uvigo.es).

This work was supported by the the European Regional Development Fund (ERDF) and the Spanish Government under projects DYNACS (TEC2010-21245-C02-02/TCM) and COMONSENS (CONSOLIDER-INGENIO 2010 CSD2008-00010), and by the Galician Regional Government under projects ESCOLMA (10TIC013CT) and "Consolidation of Research Units" 2009/62 and 2010/85.

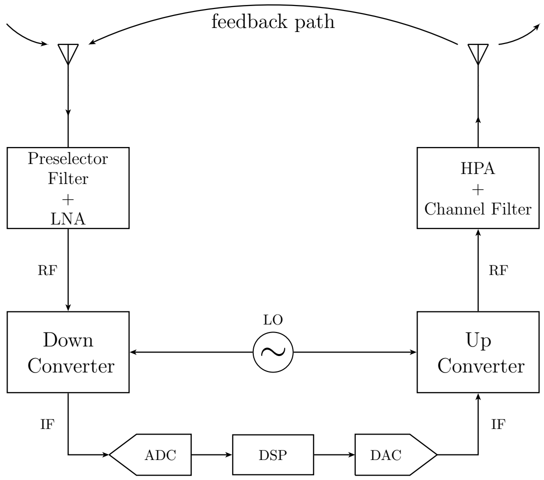

Fig. 1. Block diagram of a full-duplex relay.

[18]. These are uncorrelated with the received signal and hence allow unbiased estimation, but their insertion will degrade the signal-to-noise ratio (SNR) of the retransmitted signal. And although it may be possible to exploit pilots already embedded in the source signal [6], [19], this requires synchronization, demodulation and remodulation of the digital data, which are to be avoided in the A&F relaying approach.

In contrast, our AFC scheme hinges on a novel unsupervised adaptive filtering algorithm, which exploits knowledge of the second-order statistical information of the signal transmitted by the source and is based on the property restoral principle [13]. It does not require training sequence injection, delay insertion, or additional costly whitening filtering operations, and eliminates the bias estimation problem of the standard LMS algorithm without significantly increasing the computational complexity. Specifically, the adaptive filter adjusts the power spectral density (psd) of its output signal in order to match a prespecified 'spectral mask'. Therefore, in addition to cancelling self-interference due to antenna coupling, this scheme is also able to simultaneously and automatically compensate to some extent for phenomena such as multipath propagation in the source-relay channel and imperfections in the frequency response of the analog frontend. This equalization capability is an attractive feature, and in fact several on-channel repeater architectures have been recently proposed which include both feedback cancellation and signal equalization, albeit in different blocks, with the corresponding increase in complexity and power consumption [20]–[22].

Sec. II presents the model and discusses the bias problem. The novel AFC scheme is presented in Sec. III and analyzed in Secs. IV and V. Laboratory test results are given in Sec. VI, and Sec. VII summarizes the main conclusions. The methods discussed in this work are also described in [23].

II. Problem formulation

A. System description

The block diagram of a typical non-regenerative full-duplex relay / on-channel repeater is shown in Fig. 1. It consists of the following main components:

- The receive analog frontend, comprising the receive antenna, a downconversion stage (including pre-selection filters, low-noise amplifiers, and mixers), which retains a subband of the radio frequency (RF) spectrum containing the RF channel of interest and translates it to an intermediate frequency (IF); and an IF bandpass filter (usually a surface acoustic wave (SAW) filter), which extracts the signal of interest and rejects adjacent channels.
- A digital stage, including analog-to-digital conversion (ADC) of the IF signal at f_s samples/s, adequate processing of the resulting samples via a digital signal processor (DSP) or field-programmable gate array (FPGA), and digital-to-analog conversion (DAC) to synthesize the corresponding analog IF signal. This stage offers flexibility in order to implement functionalities such as AFC (which is the focus of this work), link quality monitoring, and digital correction of analog frontend imperfections [24].
- The transmit analog frontend, comprising an upconversion stage from IF to RF, a high-power amplifier, a channel filter to conform the RF signal to system emission masks, and the transmit antenna. A common local oscillator (LO) is used in both down- and up-conversion stages to reduce phase noise in the retransmitted signal.

Fig. 2 shows the block diagram of the equivalent discrete-time system from the point of view of the digital stage, after taking into account antenna coupling, assuming steady state and time-invariant conditions[1]. Thus, all signals involved are discrete-time IF bandpass signals with underlying sample rate f_s. The transfer functions involved are the following:

- $H(z)$ is the AFC transfer function, whose input and output signals are respectively denoted by $u(n)$ and $y(n)$;
- $G_i(z)$ and $G_o(z)$ are the discrete-time equivalent representations of the receive and transmit analog frontends, respectively;
- $F(z)$ models the feedback path due to antenna coupling;
- $C(z)$ denotes the discrete-time equivalent channel from the source to the relay.

In Fig. 2, $s(n)$ and $v(n)$ are the IF representation of the signals transmitted by the source and the relay, respectively, whereas $\eta(n)$ models the additive noise. The transfer functions $C(z)$, $F(z)$, $G_i(z)$ and $G_o(z)$ are assumed unknown, and the AFC only has access to its input and output signals $u(n)$, $y(n)$. We model $\{s(n)\}$, $\{\eta(n)\}$ as statistically independent zero-mean wide sense stationary processes with psds $\mathsf{S}_s(z)$, $\mathsf{S}_\eta(z)$ respectively.

B. AFC structure

Note that the closed-loop transfer functions from $\eta(n)$ and $s(n)$ to the AFC output $y(n)$ are respectively

$$T_{\eta y}(z) = \frac{H(z)G_i(z)}{1 - H(z)G_i(z)F(z)G_o(z)}, \quad T_{sy}(z) = C(z)T_{\eta y}(z). \tag{1}$$

Suppose that $H(z)$ is constrained to have an all-pole structure, i.e. $H(z) = b/[1 + bA(z)]$, where b is a constant and $A(z)$ is

[1]The AFC should be able to track time variations in the feedback channel if these are sufficiently slow.

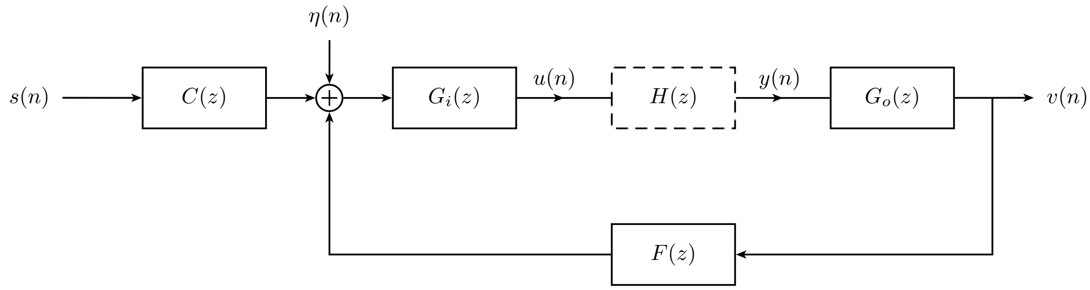

Fig. 2. Equivalent discrete-time system modeling the relay operation.

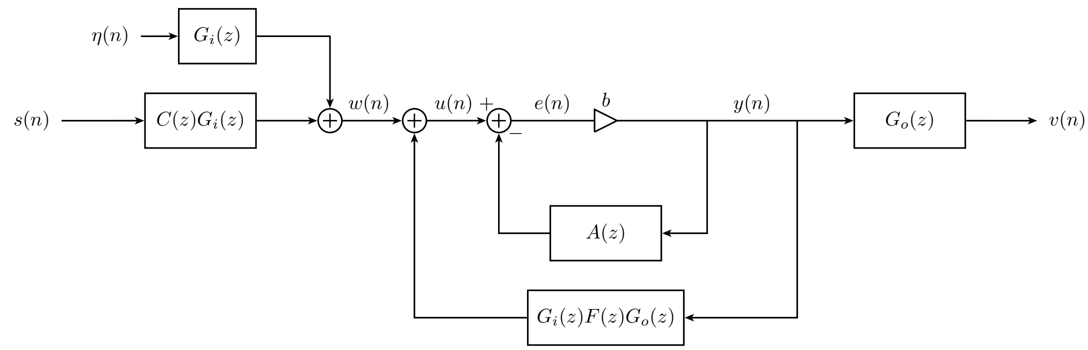

Fig. 3. Equivalent system configuration with an all-pole AFC.

strictly causal. In that case, (1) becomes

$$T_{sy}(z) = \frac{bG_i(z)C(z)}{1 + bA(z) - bG_i(z)F(z)G_o(z)}, \quad (2)$$

and therefore, by choosing $A(z) = G_o(z)G_i(z)F(z)$, the effect of the feedback is perfectly canceled, resulting in

$$T_{\eta y}(z) = bG_i(z), \qquad T_{sy}(z) = C(z)T_{\eta v}(z). \quad (3)$$

Thus, an all-pole filter is a natural candidate for the AFC, and it is the structure that will be adopted in the sequel. Fig. 3 shows an equivalent block diagram in terms of b and $A(z)$. Note that the order of $A(z)$ must be at least as large as that of the equivalent feedback path $G_i(z)F(z)G_o(z)$ in order to make cancellation feasible.

C. The bias problem

The goal is to design an effective algorithm to update the all-pole AFC coefficients. The fact that the only observable signal is $u(n)$, together with the lack of knowledge of the transfer functions involved, make this a challenging task. To clarify this issue, note that $y(n)$ can be seen as the input to the filter $A(z) = \sum_{k=1}^{M} a_k z^{-k}$ in order to form the error signal

$$e(n) = u(n) - \sum_{k=1}^{M} a_k y(n-k). \quad (4)$$

From Fig. 3, it would seem that $A(z)$ is operating in a system identification configuration [14], since it is placed in parallel with the target transfer function $G_o(z)G_i(z)F(z)$. Thus, one may consider the minimization of $E\{e^2(n)\}$ (the variance of the 'identification error') as design criterion. Assuming b fixed, and since $y(n) = be(n)$, this amounts to choosing $A(z)$ in order to minimize $E\{y^2(n)\}$. However, this approach does not lead to the desired solution, yielding a biased estimate of the feedback path. To see this, let us assume that the number of coefficients M of $A(z)$ is arbitrarily large, so that we can synthesize an arbitrary frequency response $H(e^{j\omega}) = b/[1 + bA(e^{j\omega})]$. In that case, it follows from [25] that the variance at the output of $H(z)$ is minimized iff its output $\{y(n)\}$ is a white process, i.e. its psd is constant with frequency. But since the system is operating with *bandpass* IF signals, any adaptive algorithm that attempts to minimize the variance $E\{e^2(n)\}$ will end up enhancing out-of-band noise in order to flatten the psd at the AFC output, which is clearly undesirable.

Minimization of $E\{e^2(n)\}$ by a stochastic gradient descent takes the following form [26], where $\mu > 0$ is a small stepsize:

$$a_k(n+1) = a_k(n) + \mu e(n) y_F(n-k), \quad 1 \le k \le M, \quad (5)$$

where $y_F(n-k) = -\partial e(n)/\partial a_k$ is recursively computed as

$$y_F(n) = y(n) - b\sum_{k=1}^{M} a_k(n) y_F(n-k). \quad (6)$$

Besides the bias problem, this approach also has the drawback of requiring an additional filter in order to generate the signal $y_F(n)$ as per (6). This is often sidestepped by simply using Feintuch's Pseudolinear Regression (PLR) approximation [27] $y_F(n) \approx y(n)$, which results in

$$a_k(n+1) = a_k(n) + \mu e(n) y(n-k), \quad 1 \le k \le M. \quad (7)$$

Note that (7) corresponds to the standard LMS algorithm for the adaptation of $A(z)$ that would result if one neglected the fact that the input $y(n)$ to $A(z)$ is also (a scaled version of) the identification error, and hence depends on the actual value of $A(z)$. This simplified algorithm also suffers from the bias problem: at any stationary point of (7), one must have $E\{e(n)y(n-k)\} = 0$, or equivalently, since $y(n) = be(n)$, $E\{y(n)y(n-k)\} = 0$ for $1 \le k \le M$. If the order M is sufficiently large, this implies that $\{y(n)\}$ is again a white process, and thus out-of-band noise enhancement will ensue.

A simple means to overcome the bias problem is to introduce a delay of d samples within the feedback loop of the AFC [5], whose transfer function becomes $H(z) = bz^{-d}/[1+bz^{-d}A(z)]$. In that case one has $y(n) = be(n-d)$, whereas (4) and (7) still hold. Assuming M large, the conditions at any stationary point of (7) become $E\{y(n)y(n-k)\} = 0$ for $k > d$. Thus, if d is chosen to be larger than the correlation time (in samples) of the bandpass process $\{s(n)\}$, the whitening effect at the AFC output is avoided. However, this approach increases the overall delay of the repeater by d/f_s s.

III. Spectrum Shaping algorithm

A. Derivation

In order to avoid the bias issue without increasing the overall delay, we observe that the problem with the PLR approach (7) resides in the fact that the algorithm is trying to drive the nonzero-lag autocorrelation terms of the filter output towards the zero value. However, we know that, should cancellation be achieved, and neglecting for the time being noise and multipath effects, the filter output should be a possibly scaled and delayed replica of the desired signal $\{s(n)\}$ (the sampled IF representation of the signal transmitted by the source), whose autocorrelation sequence can be assumed known. It makes sense, therefore, to attempt to shift the stationary points of the PLR scheme (7) toward the correct values by exploiting this knowledge. This can be achieved by modifying (7) into

$$a_k(n+1) = a_k(n) + \mu(y(n)y(n-k) - r_k), \quad 1 \le k \le M, \quad (8)$$

where $r_1, \ldots, r_M$ are suitable constants. The hope is that (8) will drive the output signal autocorrelation terms to the values r_k, for $k = 1, \ldots, M$. In addition, in order to set the zero-lag autocorrelation (i.e. the output power) to a given value r_0, the feedforward coefficient b is made adaptive, implementing an automatic gain control (AGC) rule:

$$b(n+1) = b(n) - \mu(y^2(n) - r_0). \quad (9)$$

A positivity constraint may be enforced on $b(n)$, since AGC loops are affected by a sign ambiguity which does not impact their performance.

B. Discussion

The choice of the constants $\{r_k\}_{k=0}^{M}$ is determined by the reference psd that one desires to obtain at the adaptive filter output upon convergence. At any stationary point of (8)-(9), the expected value of the correction terms must be zero:

$$E\{y(n)y(n-k)\} = r_k, \qquad 0 \le k \le M. \quad (10)$$

This shows that it is possible to specify the autocorrelation sequence (up to lag M) that the output process $\{y(n)\}$ will have once the filter has converged. If M is sufficiently large, this amounts to specifying the desired psd at the AFC output: the adaptive filter is effectively shaping the power spectrum of the output signal. Hence, it makes sense to choose $\{r_k\}$ as the autocorrelation sequence of the signal $\{s(n)\}$, up to an arbitrary scaling that allows to set the power at the DAC input to the desired level. In that case, if a stationary point is reached and M is sufficiently large, then the psd of $\{y(n)\}$, $\mathsf{S}_y(e^{j\omega})$, will be a scaled version of $\mathsf{S}_s(e^{j\omega})$:

$$\begin{aligned} \mathsf{S}_y &= |T_{sy}|^2\mathsf{S}_s + |T_{\eta y}|^2\mathsf{S}_\eta \\ &= |T_{\eta y}|^2\left(|C|^2\mathsf{S}_s + \mathsf{S}_\eta\right) = \beta^2\mathsf{S}_s, \end{aligned} \quad (11)$$

where β^2 is a scaling constant. From (11), and letting $\Gamma(e^{j\omega}) \doteq \mathsf{S}_s(e^{j\omega})/\mathsf{S}_\eta(e^{j\omega})$, the transfer functions at the stationary point are obtained:

$$|T_{\eta y}|^2 = \frac{\beta^2\Gamma}{1+|C|^2\Gamma}, \quad |T_{sy}|^2 = \frac{\beta^2|C|^2\Gamma}{1+|C|^2\Gamma}. \quad (12)$$

Suppose now that the input spectral SNR is sufficiently high, i.e. $|C(e^{j\omega})|^2\Gamma(e^{j\omega}) \gg 1$, so that we can neglect the noise. From (12), this results in $|T_{sy}(e^{j\omega})|^2 \approx \beta^2$, that is,

$$T_{sy}(z) = \frac{bG_i(z)C(z)}{1 + bA(z) - bG_i(z)F(z)G_o(z)}, \quad (13)$$

must be an allpass transfer function. Suppose that the effective feedforward and feedback paths, $bG_i(z)C(z)$ and $bG_i(z)F(z)G_o(z)$ respectively, can be modeled as finite impulse response (FIR) filters of order no larger than M. In addition, suppose that $G_i(z)C(z)$ is minimum phase. In that case, it is clear that the allpass system $T_{sy}(z)$ in (13) must reduce to a pure delay, i.e. the adaptive filter is simultaneously canceling the unwanted feedback *and* equalizing the effective source-relay channel (which includes the wireless channel and the linear distortion introduced by the receive analog frontend). If $G_i(z)C(z)$ is not minimum phase (for example, due to pre-echoes present in the wireless multipath environment), the all-pole structure of the AFC cannot equalize the phase of the effective channel, but only its magnitude, resulting in an allpass characteristic of the overall system; this, of course, is due to the fact that only second-order statistical information about the desired signal $\{s(n)\}$ is being exploited.

Observe that in order to completely determine the desired psd (up to a scaling), in general it does not suffice to specify the autocorrelation sequence $\{r_k\}$ for $k \ge 1$; the zero-lag term r_0 must be given as well. This makes the introduction of the AGC (9) necessary; the exception is the case in which $r_k = 0$ for $k \ne 0$, which is the reason why the original PLR scheme (7) can operate with fixed b. Finally, note that the computational complexity of the modified algorithm (8)-(9) is practically the same as that of the PLR update rule (7).

C. Noise analysis

In order to gauge the behavior of the proposed design in noisy settings, consider the SNR at the AFC output, given by

$$\text{SNR}_{\text{out}} \doteq \frac{\frac{1}{2\pi}\int_{-\pi}^{\pi}|T_{sy}|^2\mathsf{S}_s d\omega}{\frac{1}{2\pi}\int_{-\pi}^{\pi}|T_{\eta y}|^2\mathsf{S}_\eta d\omega}. \quad (14)$$

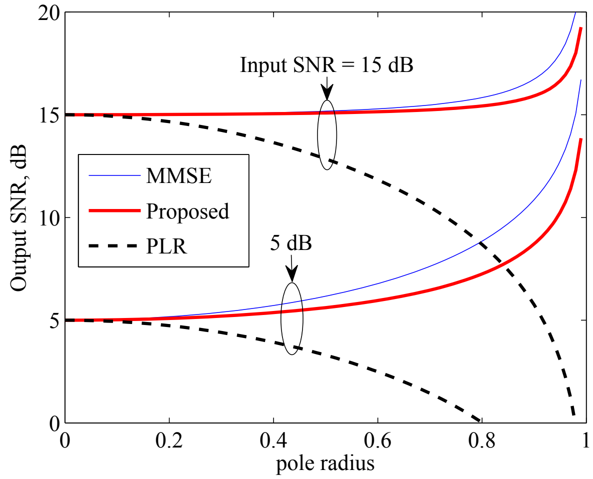

Fig. 4. Output SNR with white noise and a first-order AR process.

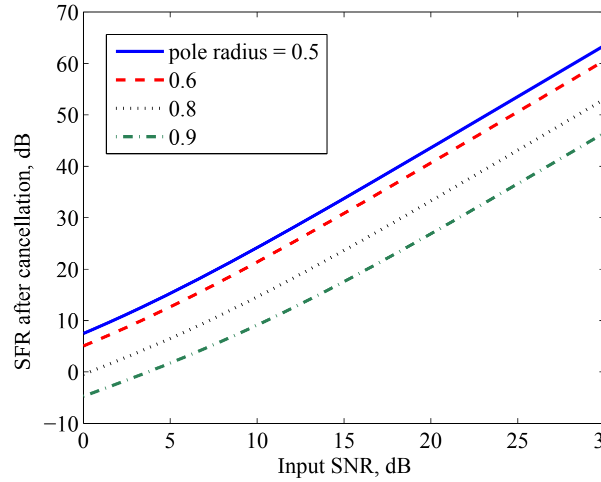

Fig. 5. Post-cancellation Signal-to-Feedback Ratio with white noise and a first-order AR process.

For the proposed approach, $|T_{\eta y}|^2$, $|T_{sy}|^2$ are given by (12), whereas for a staionary point of the PLR scheme they can be obtained from $\mathsf{S}_y = \beta^2$, which yields

$$|T_{\eta y}|^2 = \frac{\beta^2}{1+|C|^2\Gamma}\mathsf{S}_\eta^{-1}, \quad |T_{sy}|^2 = \frac{\beta^2|C|^2}{1+|C|^2\Gamma}\mathsf{S}_\eta^{-1}. \quad (15)$$

We also consider the Minimum Mean Square Error (MMSE) design in which $T_{\eta y}$ and $T_{sy} = CT_{\eta y}$ are chosen to minimize $E\{|y(n) - \beta s(n)|^2\}$, resulting in

$$|T_{\eta y}|^2 = \frac{\beta^2|C|^2\Gamma^2}{(1+|C|^2\Gamma)^2}, \quad |T_{sy}|^2 = \beta^2\left(\frac{|C|^2\Gamma}{1+|C|^2\Gamma}\right)^2. \quad (16)$$

Note that an MMSE AFC would require the availability of $\{s(n)\}$; thus, it can be considered as a benchmark for blind designs such as PLR and the proposed approach. In Fig. 4 the three designs are compared in terms of SNR_{out} when S_η is constant (white noise), the channel $|C|^2$ is constant, and

$$\mathsf{S}_s(e^{j\omega}) = \frac{1}{1+\rho^2-2\rho\cos\omega} \quad (17)$$

corresponds to the psd of a first-order autoregressive (AR) process with pole at ρ. The input SNR is given by

$$\text{SNR}_{\text{in}} \doteq \frac{\frac{1}{2\pi}\int_{-\pi}^{\pi}|C(e^{j\omega})|^2\mathsf{S}_s(e^{j\omega})d\omega}{\frac{1}{2\pi}\int_{-\pi}^{\pi}\mathsf{S}_\eta(e^{j\omega})d\omega}. \quad (18)$$

For $\rho = 0$ the desired signal $\{s(n)\}$ is white and the three designs coincide. However, as $|\rho|$ increases so that $\{s(n)\}$ becomes more colored, the PLR approach suffers from a significant SNR loss due to the noise enhancement problem. The proposed approach, in contrast, is able to provide an improvement in terms of output SNR; though suboptimal, it follows the same trend as the non-blind MMSE design, with a gap that narrows as the input SNR increases. This example is illustrative of the noise behavior of the proposed design in more general scenarios.

IV. Analysis of an M-th order canceller

The study of the convergence properties of the spectrum shaping algorithm (8)-(9) in general settings is difficulted by the recursive structure of the adaptive filter. Next we provide an analysis in terms of the properties of stationary points for a particular case: a sufficiently long adaptive filter, operating in a "cancellation-only" configuration, meaning that the linear distortion introduced by the propagation channel and the analog frontend can be neglected. In that situation, and assuming that the noise can be neglected, the following result holds; see Appendix A for the proof.

Theorem 1. *Assume that $\eta(n) = 0$, $C(z)G_i(z) = 1$, and that the AFC order M is no less than that of the feedback path $G_i(z)F(z)G_o(z)$. Let $\mathsf{S}_s(e^{j\omega})$ be the psd of $\{s(n)\}$. If $\mathsf{S}_s(e^{j\omega})$ is bounded and nonzero for all ω, and the constants $\{r_k\}_{k=0}^M$ are chosen as $r_k = \beta^2 E\{s(n)s(n-k)\}$ for some $\beta > 0$, then the point $(b_\star, A_\star(z))$ given by*

$$b_\star = \beta, \quad A_\star(z) = G_i(z)F(z)G_o(z), \quad (19)$$

is a (locally) convergent stationary point in mean of the adaptive algorithm (8)-(9).

In other words, when the only mission of the adaptive filter is to cancel the unwanted feedback and no equalization is required in order to restore the reference autocorrelation at the output, the desired parameter values yielding perfect cancellation constitute a stationary point of the adaptive scheme, and moreover, the algorithm will drive the parameters (in mean) to these desired values if the starting point is sufficiently close (and the stepsize is sufficiently small).

Consider now the same "cancellation-only" setting, but taking the noise $\eta(n)$ into account. The adaptive algorithm will drive the AFC towards a point at which the output psd will satisfy $\mathsf{S}_y(e^{j\omega}) = \beta^2\mathsf{S}_s(e^{j\omega})$, provided that M is sufficiently large. This results in

$$\frac{b^2}{|1+b(A-G_iFG_o)|^2} = \frac{\beta^2\mathsf{S}_s}{\mathsf{S}_s+\mathsf{S}_\eta}, \quad (20)$$

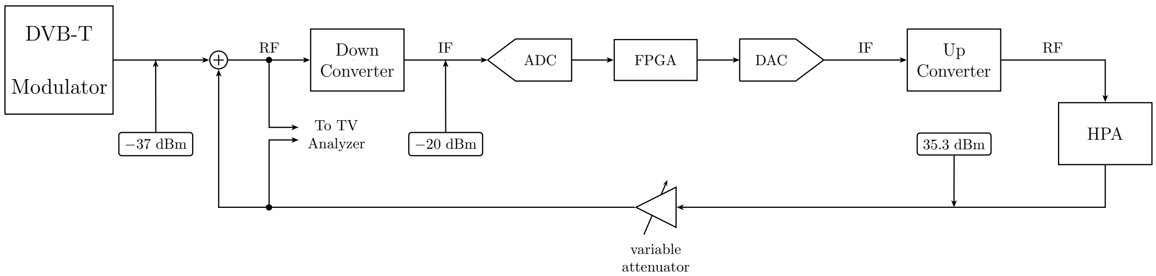

Fig. 6. Block diagram of the experimental setup.

whose solution will be biased away from the "perfect cancellation" setting (19) due to the presence of the S_η term in the right-hand side of (20). Therefore there will be some residual coupling, which can be gauged by the post-cancellation Signal-to-Feedback Ratio (SFR), i.e. the ratio of the powers of the desired and feedback components after cancellation. Fig. 5 shows this ratio for a white noisy setting with a first-order AR process $\{s(n)\}$ with pole at ρ, i.e. S_s as in (17), in terms of the input SNR. Derivation details are given in Appendix B, concluding that for high SNR_{in},

$$\text{SFR} \approx \text{SNR}_{\text{in}}^2 \left(\frac{1-\rho^2}{\rho} \right)^2. \tag{21}$$

Thus the SFR behaves quadratically with SNR_{in} (slope 2 in log-log scale). For a given SNR_{in}, the SFR degrades as the input process becomes more colored (i.e. for a larger pole radius $|\rho|$); note that for $\rho = 0$ the right-hand side of (20) becomes constant with ω and the bias disappears, resulting in $\text{SFR} \to \infty$ as reflected in (21).

Determining the stability properties of the stationary point in these noisy settings is a difficult task. The following section provides some steps in this direction for the particular case of a first-order AFC.

V. Analysis of a first-order spectrum shaper

In this section we relax the "cancellation-only" and noiseless assumptions made in Sec. IV, but in order to make the analysis tractable we consider a first-order filter ($M = 1$) with a first-order feedback path. In the setting of Fig. 3, this amounts to having $A(z) = az^{-1}$ and $G_i(z)F(z)G_o(z) = qz^{-1}$. The system is governed by the following equations:

$$u(n) = w(n) + qy(n-1), \tag{22}$$

$$y(n) = b(n)u(n) - b(n)a(n)y(n-1), \tag{23}$$

$$b(n+1) = b(n) - \mu(y^2(n) - r_0), \tag{24}$$

$$a(n+1) = a(n) + \mu(y(n)y(n-1) - r_1). \tag{25}$$

We assume that $\{r_0, r_1\}$ are drawn from a valid autocorrelation sequence, i.e., $r_0 > 0$ and $|\alpha| < 1$, with $\alpha \doteq \frac{r_1}{r_0}$.

A. Existence of stationary points

From (22)-(23), the closed-loop system reduces for fixed values of b, a to a first-order system with pole $p = b(q-a)$:

$$y(n) = bw(n) + py(n-1), \tag{26}$$

which is stable iff $|p| < 1$.

Since no assumptions have been made so far on the input process $\{w(n)\}$ (in particular, noise may be present), the question of whether the algorithm (24)-(25) admits a stationary point is not trivial. This is addressed by the following result, whose proof can be found in Appendix C.

Lemma 1. *Let $\mathsf{S}_w(e^{j\omega})$ be the psd of $\{w(n)\}$. If $\mathsf{S}_w(e^{j\omega})$ is bounded and nonzero for all ω, then the adaptive algorithm (24)-(25) admits a stationary point corresponding to a stable closed-loop system.*

B. Analysis for first-order MA inputs

Lemma 1 guarantees the existence of stationary points under mild conditions on the input psd. We focus now on the particular case of a first-order moving average, or MA(1), input process, for which stronger results can be developed. Recall that if $\{w(n)\}$ is MA(1), then $\gamma_k \doteq E\{w(n)w(n-k)\}$ equals zero for $|k| > 1$.

Lemma 2. *Let $\{w(n)\}$ be an MA(1) process. Then there is a single stationary point $(b_\star, a_\star)$ of (24)-(25) with $b_\star > 0$ and yielding a stable closed-loop system. In addition, this stationary point is locally convergent in mean.*

The proof is given in Appendix D. Empirical evidence suggests that these results can be extended to more general settings (arbitrary order M, input psd $\mathsf{S}_w(z)$, and feedback path), although deriving formal proofs remains an open issue.

VI. Results

The proposed AFC has been tested in the laboratory. The implemented hardware module consists of a software development kit, including the input ADC, an FPGA, and the output DAC. The experimental setup is shown in Fig. 6. The signal to process is a 8-MHz OFDM digital TV signal generated according to the DVB-T standard [28], with a carrier frequency of 842 MHz and power level -37 dBm. An analog receiver frontend downconverts the RF signal (with feedback added) to an IF of 36.15 MHz. The sampling frequency and resolution of both the ADC and the DAC are 90 Msps and 14 bits respectively. In order to reduce the number of required AFC taps, the input stream is downsampled by a factor of 3 in the FPGA, so that the effective sampling rate is 30 Msps and the effective digital IF is 6.15 MHz. The AFC output is upsampled, also by a factor of 3, and a digital bandpass filter

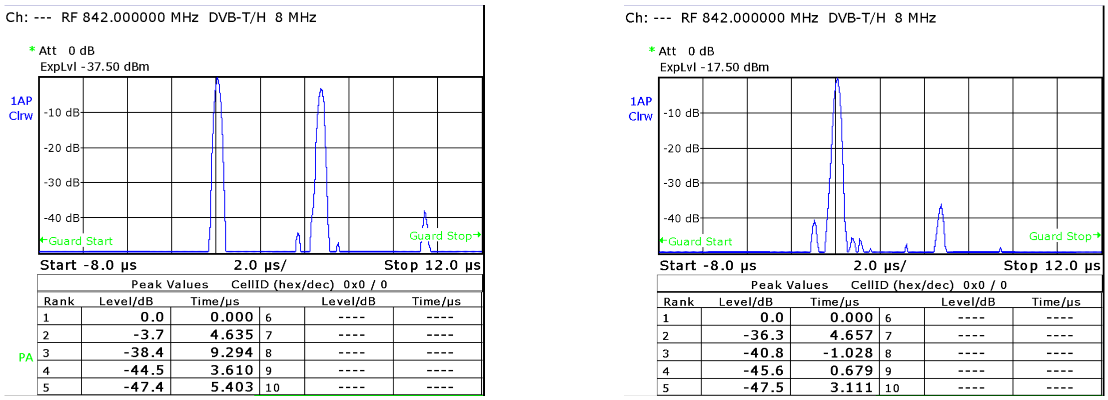

(a) Relay input (b) Relay output

Fig. 7. Echo patterns, Gain Margin $= 4$ dB.

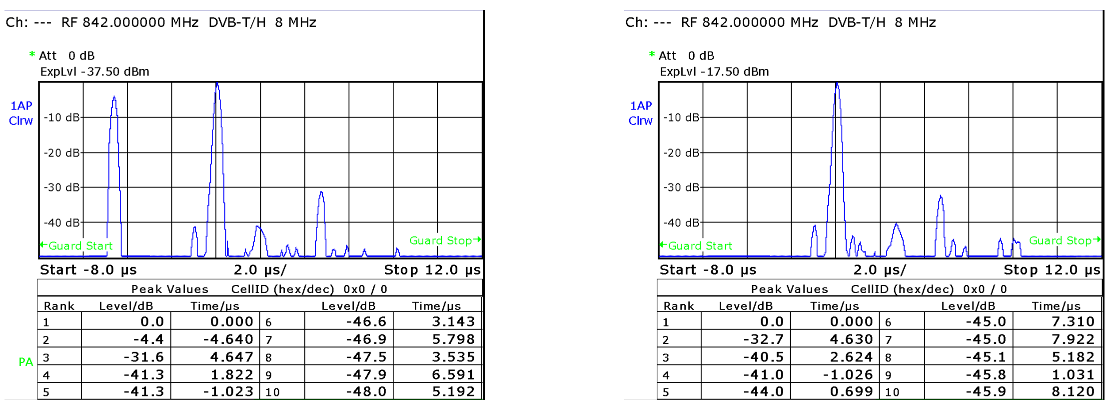

(a) Relay input (b) Relay output

Fig. 8. Echo patterns, Gain Margin $= -4$ dB.

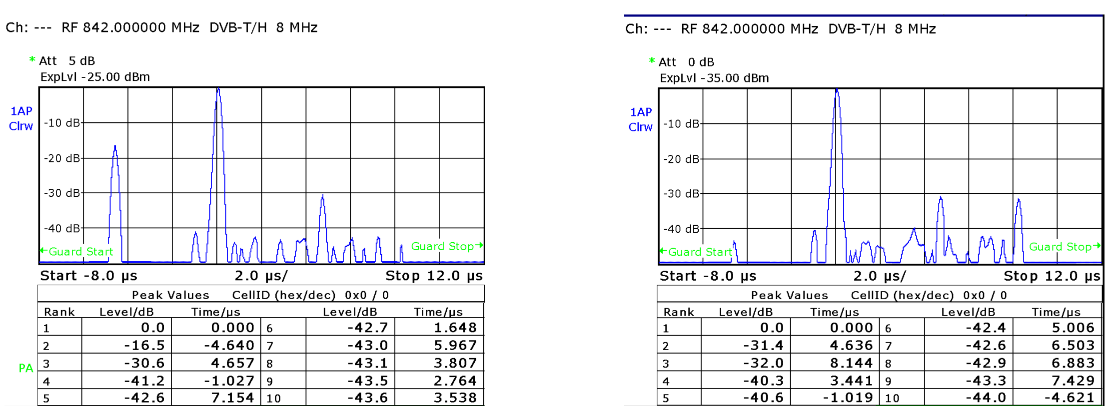

(a) Relay input (b) Relay output

Fig. 9. Echo patterns, Gain Margin $= -16$ dB.

centered at 36.15 MHz is then applied. Its output is fed to the DAC to synthesize the IF signal, which in turn is upconverted to 842 MHz and amplified, with an output power of 35.3 dBm. This RF signal is attenuated and combined with the one from the DVB-T modulator. The input and output RF signals are fed to a TV analyzer (Rohde&Schwarz ETL).

The overall delay in the feedback path of the setup is approximately 4.6 μs. Accordingly, the number of AFC taps is set to $M = 160$. Each coefficient a_k is updated only once every M sample periods, in a sequential manner, in order to alleviate the computational requirements in the FPGA (at the cost of a slower convergence rate). Since the bandpass input does not fully excite all the modes of the adaptive algorithm, coefficient drift may occur, and hence a small coefficient leakage [13] is introduced in the adaptation. The reference sequence $\{r_k\}$ was computed beforehand by estimating the

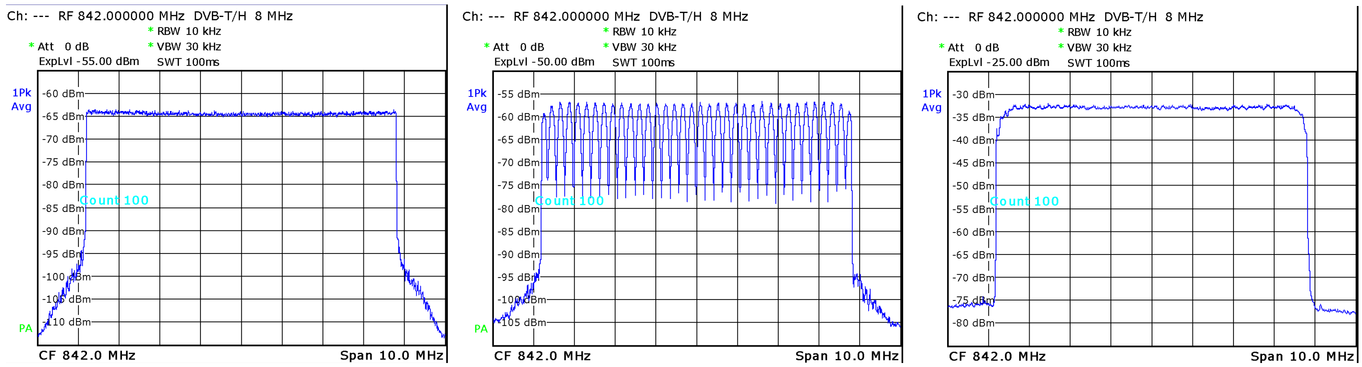

(a) Modulator output (b) Relay input (c) Relay output

Fig. 10. Power spectral densities, Gain Margin = 0 dB.

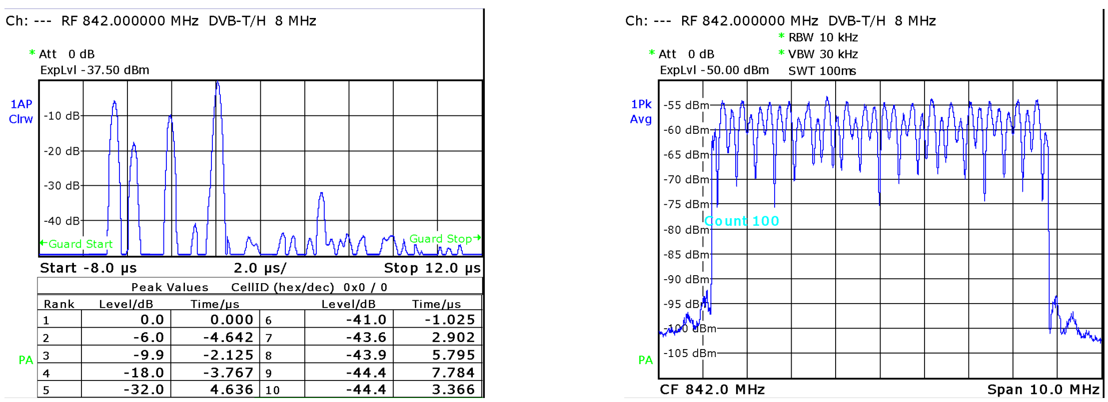

(a) Echo pattern (b) Power spectral density

Fig. 11. Signal characteristics at the relay input under multipath propagation and GM = -4 dB.

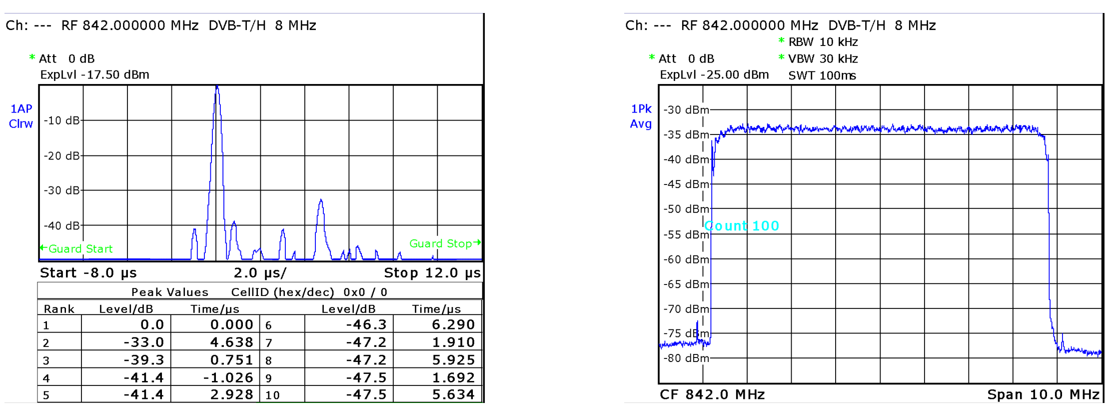

(a) Echo pattern (b) Power spectral density

Fig. 12. Signal characteristics at the relay output under multipath propagation and GM = -4 dB.

autocorrelation of a 'clean' DVB-T signal centered at 6.15 MHz from a very long record of samples at 30 Msps.

Figs. 7-9 show the steady-state echo patterns at the input and output of the relay (i.e. channel impulse responses from the DVB-T modulator to each of these two ports), as determined by the TV analyzer, for different values of the Gain Margin (GM), defined as the ratio of the powers of the desired to undesired components of the relay input signal. In the setting of Fig. 6, one has GM (dB) = -37 dBm -35.3 dBm $+A$ dB, where A is the variable attenuation in the feedback path. The GM value can also be inferred from the relative levels of the two peaks observed at the relay input echo pattern (notice that the TV analyzer always locks to the strongest component in order to set the time reference; with negative GM values, this component corresponds to the feedback path, as in Figs. 8-9). Note that the output echo patterns exhibit a single dominant peak and all residual echos have been attenuated at least 30 dB below this main path, meaning that the coupling has been effectively canceled. Stable operation was observed with GM values down to -20 dB. The effect of the AFC in the frequency domain for GM $= 0$ dB can be seen in Fig. 10. The input psd has ripples whose period is the inverse of the feedback path delay (≈ 0.22 MHz). The retransmitted signal, on the other hand, exhibits a remarkably flat psd, as desired.

Finally, in order to confirm the spectrum shaping capabilities of the novel scheme, multipath propagation conditions were artificially introduced in the desired signal before reaching the combiner at the relay input (the DVB-T modulator has the capability to simulate multipath channels with configurable delay, amplitude and phase values). A (minimum phase) three-path channel with relative delays 0, 0.9 and 2.5 μs and attenuations 0, -12 and -4 dB was considered, and the GM was set to -4 dB. As seen in Figs. 11-12, the proposed AFC effectively restores the original signal spectrum.

VII. Conclusions

We have presented a novel blind, second-order statistics based, computationally simple adaptive feedback canceller for amplify-and-forward full-duplex relays, which effectively shapes the psd of its output in terms of a prespecified spectral mask. Laboratory tests of an FPGA-based implementation show that the proposed scheme is able to effectively mitigate input-output coupling as well as minimum phase multipath distortion, without introducing significant delay. The main obstacles for a convergence analysis for arbitrary orders and settings reside in the recursive nature of the filter and in the fact that the adaptive algorithm is not an stochastic gradient descent of a meaningful cost function. Nevertheless, the presented analytical results, together with the experimental evidence, are encouraging in this respect.

Acknowledgment

The authors appreciate the help provided by Julián Martínez Soutiño and Yolanda Rodríguez Vaqueiro with the hardware implementation of the adaptive feedback canceller.

Appendix A
Proof of Theorem 1

Let $G_i(z)F(z)G_o(z) = \sum_{k=1}^{M} q_k z^{-k}$. Under the assumptions of the theorem, the signal model becomes

$$u(n) = s(n) + \sum_{k=1}^{M} q_k y(n-k), \quad (27)$$

$$y(n) = b(n)u(n) - b(n)\sum_{k=1}^{M} a_k(n) y(n-k). \quad (28)$$

Defining $\theta_0(n) \doteq b(n)$, $\theta_k(n) \doteq q_k - a_k(n)$, $1 \le k \le M$, it follows from (27)-(28) that

$$y(n) = \theta_0(n)s(n) + \theta_0(n)\sum_{k=1}^{M} \theta_k(n) y(n-k). \quad (29)$$

Let $\boldsymbol{\theta} \doteq [\ \theta_0 \quad \theta_1 \quad \cdots \quad \theta_M\ ]^T$. It is clear that for $\boldsymbol{\theta} = \boldsymbol{\theta}_\star \doteq [\ \beta \quad 0 \quad \cdots \quad 0\ ]^T$, one has $y(n) = \beta s(n)$ and therefore the conditions (10) hold, showing that $\boldsymbol{\theta}_\star$ is a stationary point.

To show local convergence, we resort to the ordinary differential equation (ODE) method. Under some general conditions [26], the trajectories of (8)-(9) converge in some probabilistic sense as $\mu \to 0$ to the solution of the ODE

$$\frac{d\boldsymbol{\theta}(t)}{dt} = \begin{bmatrix} f_0(\boldsymbol{\theta}) \\ f_1(\boldsymbol{\theta}) \\ \vdots \\ f_M(\boldsymbol{\theta}) \end{bmatrix}, \quad f_k(\boldsymbol{\theta}) \doteq r_k - E\{y(n)y(n-k)\}, \quad (30)$$

where the expectations are evaluated at $\boldsymbol{\theta} = \boldsymbol{\theta}(t)$. The stationary point $\boldsymbol{\theta}_\star$ is locally convergent iff the eigenvalues of the matrix $\boldsymbol{A}(\boldsymbol{\theta}_\star)$ all have negative real parts, where $[\boldsymbol{A}(\boldsymbol{\theta})]_{kl} \doteq \partial f_k(\boldsymbol{\theta})/\partial\theta_l$.

Let $\delta_l(n) \doteq \partial y(n)/\partial\theta_l$. Then, from (30),

$$\frac{\partial f_k(\boldsymbol{\theta})}{\partial\theta_l} = -\left(E\{\delta_l(n)y(n-k)\} + E\{y(n)\delta_l(n-k)\}\right). \quad (31)$$

From (29), it follows that for fixed values of the parameters,

$$\delta_0(n) = \frac{1}{\theta_0} y(n) + \theta_0 \sum_{i=1}^{M} \theta_i \delta_0(n-i), \quad (32)$$

$$\delta_l(n) = \theta_0 y(n-l) + \theta_0 \sum_{i=1}^{M} \theta_i \delta_l(n-i), \quad (33)$$

for $l = 1, \ldots, M$. Hence, for $\boldsymbol{\theta} = \boldsymbol{\theta}_\star$ (yielding $y(n) = \beta s(n)$) the derivative signals (32)-(33) evaluate to

$$\delta_0(n) = \frac{1}{\beta} y(n) = s(n), \quad (34)$$

$$\delta_l(n) = \beta y(n-l) = \beta^2 s(n-l), \quad 1 \le l \le M, \quad (35)$$

and therefore the desired elements of $\boldsymbol{A}(\boldsymbol{\theta}_\star)$ are given by

$$\frac{\partial f_k(\boldsymbol{\theta}_\star)}{\partial\theta_0} = -2\beta E\{s(n)s(n-k)\} = -2\beta^{-1} r_k, \quad (36)$$

$$\begin{aligned}\frac{\partial f_k(\boldsymbol{\theta}_\star)}{\partial\theta_l} &= -\beta^3\left(E\{s(n-l)s(n-k)\} + E\{s(n)s(n-k-l)\}\right) \\ &= -\beta(r_{k-l} + r_{k+l}), \quad 1 \le l \le M, \quad (37)\end{aligned}$$

so that we can write $\boldsymbol{A}(\boldsymbol{\theta}_\star) = -\beta^{-1}(\boldsymbol{T}+\boldsymbol{H})\boldsymbol{D}^2$, with

$$[\boldsymbol{T}]_{kl} = r_{k-l}, \quad [\boldsymbol{H}]_{kl} = r_{k+l}, \quad \boldsymbol{D} = \begin{bmatrix} 1 & \\ & \beta\boldsymbol{I} \end{bmatrix}. \quad (38)$$

Note that $\boldsymbol{T}$ is symmetric Toeplitz, whereas $\boldsymbol{H}$ is symmetric Hankel. Although $\boldsymbol{A}(\boldsymbol{\theta}_\star)$ is not symmetric for $\beta \neq 1$, its eigenvalues are the same as those of

$$\boldsymbol{D}\boldsymbol{A}(\boldsymbol{\theta}_\star)\boldsymbol{D}^{-1} = -\beta^{-1}\boldsymbol{D}(\boldsymbol{T}+\boldsymbol{H})\boldsymbol{D}, \quad (39)$$

which is symmetric and therefore has real eigenvalues. We now apply the following result from [29]: if the Fourier Transform of the autocorrelation sequence $\{r_k\}_{k=-\infty}^{\infty}$ is positive at all frequencies, then $\boldsymbol{T}+\boldsymbol{H}$ is positive definite. Since in our case this transform is $\beta^2 \mathsf{S}_s(e^{j\omega})$ which is positive for all ω by assumption, the result holds, and it follows that the matrix in (39) is negative definite, concluding the proof.

Appendix B
SFR computations

We assume a "cancellation-only" setting with white noise, i.e. $\mathsf{S}_\eta(e^{j\omega}) = \sigma_\eta^2$, and a first-order AR process $\{s(n)\}$ with psd given by (17). The input SNR is given by

$$\text{SNR}_{\text{in}} = \frac{E\{s^2(n)\}}{\sigma_\eta^2} = \frac{1}{(1-\rho^2)\sigma_\eta^2}. \quad (40)$$

From (20), it follows that the stationary point of the adaptive algorithm must satisfy

$$\frac{b^2}{|1+b(A-G_iGG_o)|^2} = \frac{\beta^2}{1+\sigma_\eta^2(1-\rho z)(1-\rho z^{-1})} \quad (41)$$

at $z = e^{j\omega}$. Hence, the resulting closed-loop system as a single pole, i.e. $1 + b(A - G_iFG_o) = 1 - pz^{-1}$ where p is the root of $1 + \sigma_\eta^2(1-\rho z)(1-\rho z^{-1})$ with $|p| < 1$:

$$p = \text{sign}(\rho)\frac{\kappa - \sqrt{\kappa^2-4}}{2}, \quad \kappa \doteq \frac{\text{SNR}_{\text{in}}(1-\rho^2)+1+\rho^2}{|\rho|}, \quad (42)$$

whereas the value of b^2 is given by

$$b^2 = \beta^2\frac{1-\rho^2}{|\rho|}|p| \cdot \text{SNR}_{\text{in}}. \quad (43)$$

The residual feedback signal is thus given by $-\frac{p}{b}y(n-1)$, whose power is $\frac{p^2}{b^2}E\{y^2(n-1)\} = \frac{p^2}{b^2}\beta^2 E\{s^2(n)\}$. Then

$$\text{SFR} = \frac{E\{s^2(n)\}}{\frac{p^2}{b^2}E\{y^2(n-1)\}} = \frac{1-\rho^2}{|\rho|\cdot|p|}\text{SNR}_{\text{in}}. \quad (44)$$

For large SNR_{in}, one has from (42) that

$$\kappa \approx \text{SNR}_{\text{in}}\frac{1-\rho^2}{|\rho|}, \quad |p| \approx \frac{1}{\kappa}, \quad (45)$$

which, when substituted in (44), yield (21).

Appendix C
Proof of Lemma 1

Consider the closed-loop system (26) obtained for fixed values of a and b. Multiplying (26) by $y(n-1)$ and taking expected values,

$$E\{y(n)y(n-1)\} = bE\{w(n)y(n-1)\} + pE\{y^2(n-1)\}. \quad (46)$$

Let $x(n) = w(n) + px(n-1)$, so that $y(n) = bx(n)$. At a stationary point $(b_\star, a_\star)$ of the adaptive algorithm (24)-(25), one must have, with $p_\star = b_\star(q - a_\star)$,

$$r_0 = b_\star^2 E\{x^2(n)\}, \quad (47)$$
$$r_1 = b_\star E\{w(n)y(n-1)\} + p_\star r_0, \quad (48)$$

where the expectations are evaluated at $(b_\star, a_\star)$. With $\alpha = \frac{r_1}{r_0}$, let $\mathcal{F} : (-1,1) \to \mathbb{R}$ be defined by

$$\mathcal{F}(p) = \alpha - \frac{E\{w(n)x(n-1)\}}{E\{x^2(n)\}}. \quad (49)$$

Then it is seen that the stationary points (in terms of the pole parameter p, as the right-hand side of (49) does not depend on b) are fixed points of $\mathcal{F}$, i.e. $p_\star = \mathcal{F}(p_\star)$. Now note that

$$E\{x^2(n)\} = \frac{1}{2\pi}\int_{-\pi}^{\pi}\frac{\mathsf{S}_w(e^{j\omega})}{|1-pe^{j\omega}|^2}d\omega, \quad (50)$$

which goes to infinity as $p \to \pm 1$, since $\mathsf{S}_w(e^{j\omega}) > 0$ for all ω. On the other hand,

$$E\{w(n)x(n-1)\} = \frac{1}{2\pi j}\oint_{|z|=1}\frac{\mathsf{S}_w(z)}{1-pz}dz. \quad (51)$$

For $|p| < 1$, the only poles of the integrand inside the unit circle are those of $\mathsf{S}_w(z)$; hence, using the residue theorem to evaluate (51), it is seen that this quantity remains finite even as p approaches ± 1. Hence,

$$\lim_{p\to\pm 1}\frac{E\{w(n)x(n-1)\}}{E\{x^2(n)\}} = 0, \quad (52)$$

so that $\lim_{p\to\pm1}\mathcal{F}(p) = \alpha$. Hence we can continuously extend the domain of $\mathcal{F}$ in order to include the points $p = \pm 1$ upon defining $\mathcal{F}(\pm 1) = \alpha$. Since $|\alpha| < 1$ and $\mathcal{F}$ is continuous in $[-1, 1]$, direct application of the Mean Value Theorem shows that there must exist a $p_\star \in (-1, 1)$ such that $\mathcal{F}(p_\star) - p_\star = 0$. The corresponding values $(b_\star, a_\star)$ are then

$$b_\star = \sqrt{\frac{r_0}{E\{x^2(n)\}|_{p=p_\star}}}, \qquad a_\star = q - \frac{p_\star}{b_\star}. \quad (53)$$

Appendix D
Proof of Lemma 2

Let us rewrite (26) as

$$y(n) = b\sum_{k=0}^{\infty}p^k w(n-k). \quad (54)$$

If $\{w(n)\}$ is MA(1), then from (54) it is readily seen that

$$E\{w(n)y(n)\} = b(\gamma_0 + p\gamma_1), \quad (55)$$
$$E\{w(n)y(n-1)\} = b\gamma_1. \quad (56)$$

On the other hand, from (26) one has

$$E\{y^2(n)\} = bE\{w(n)y(n)\} + pE\{y(n)y(n-1)\}, \quad (57)$$
$$E\{y(n)y(n-1)\} = bE\{w(n)y(n-1)\} + pE\{y^2(n-1)\}. \quad (58)$$

Substituting (55)-(56) in (57)-(58), and taking into account that at a stationary point $(b_\star, p_\star)$ it must hold that $E\{y(n)y(n-k)\} = r_k$ for $k \in \{0, 1\}$, one has

$$r_0 = b_\star^2(\gamma_0 + p_\star\gamma_1) + p_\star r_1, \quad (59)$$
$$r_1 = b_\star^2\gamma_1 + p_\star r_0. \quad (60)$$

Multiplying (59) by $\gamma_1/(\gamma_0 r_0)$ and using (60), one obtains

$$\rho p_\star^2 + (1 - 2\alpha\rho)p_\star + (\rho - \alpha) = 0, \quad (61)$$

where $\rho \doteq \frac{\gamma_1}{\gamma_0}$. Note that $|\alpha| = \frac{|r_1|}{r_0} < 1$ by assumption. On the other hand, it is readily checked that $|\rho| < \frac{1}{2}$ if $\{w(n)\}$ is MA(1). Define the second-order polynomial $P(p) = \rho p^2 + (1-2\alpha\rho)p + (\rho - \alpha)$. Then from (61), any stationary point $p_\star$ is a root of P. Since $P(1)P(-1) = -(1-\alpha^2)(1-4\rho^2) < 0$, it follows that there is one and only one root $p_\star$ in $(-1, 1)$. The corresponding values of $(b_\star, a_\star)$ are then given by (53).

To show local convergence, we resort again to the ODE method. In this case the corresponding ODE is given by

$$\begin{bmatrix}\dot{b}\\ \dot{a}\end{bmatrix} = \begin{bmatrix}E\{y^2(n)\} - r_0\\ r_1 - E\{y(n)y(n-1)\}\end{bmatrix} \doteq \begin{bmatrix}f_0(b,a)\\ f_1(b,a)\end{bmatrix}, \quad (62)$$

where the expectations are evaluated at $(b, a) = (b(t), a(t))$. From (54), it follows that

$$E\{y^2(n)\} = \frac{b^2\gamma_0}{1-p^2}(1+2\rho p), \quad (63)$$

$$E\{y(n)y(n-1)\} = \frac{b^2\gamma_0}{1-p^2}(\rho + p + \rho p^2). \quad (64)$$

A stationary point $(b_\star, a_\star)$ is locally convergent in mean iff the eigenvalues of $\boldsymbol{A}(b_\star, a_\star)$ have negative real parts, where

$$\boldsymbol{A}(b,a) \doteq \begin{bmatrix} \frac{\partial f_0(b,a)}{\partial b} & \frac{\partial f_0(b,a)}{\partial a} \\ \frac{\partial f_1(b,a)}{\partial b} & \frac{\partial f_1(b,a)}{\partial a} \end{bmatrix} = \frac{-b\gamma_0}{(1-p^2)^2}\boldsymbol{C}(b,a), \quad (65)$$

and with $\boldsymbol{C}(b,a)$ defined as

$$\boldsymbol{C}(b,a) = \begin{bmatrix} 2(-\rho p^3 + 3\rho p + 1) & -2b^2(\rho p^2 + p + \rho) \\ 2\rho p^4 + p^3 - 4\rho p^2 - 3p - 2\rho & b^2(p^2 + 4\rho p + 1) \end{bmatrix} (66)$$

In view of (65), since $b_\star > 0$, a necessary and sufficient condition for local convergence is that $\det \boldsymbol{C}(b_\star, a_\star) > 0$ and $\operatorname{tr} \boldsymbol{C}(b_\star, a_\star) > 0$. One has

$$\det \boldsymbol{C}(b,a) = 2b^2(1-p^2)^2[1 - 2\rho(\rho - p - \rho p^2)]. \quad (67)$$

The term in brackets in (67) is positive for all $|p| < 1$, $|\rho| < \frac{1}{2}$. Thus $\det \boldsymbol{C}(b_\star, a_\star) > 0$. Also, the diagonal terms of $\boldsymbol{C}(b,a)$ are positive for all $|p| < 1$, $|\rho| < \frac{1}{2}$. Thus $\operatorname{tr} \boldsymbol{C}(b_\star, a_\star) > 0$, and local convergence follows.

References

[1] R. Pabst, B. H. Walke, D. C. Schultz, P. Herhold, H. Yanikomeroglu, S. Mukherjee, H. Viswanathan, M. Lott, W. Zirwas, M. Dohler, H. Aghvami, D. D. Falconer, and G. P. Fettweis, "Relay-based deployment concepts for wireless and mobile broadband radio," *IEEE Commun. Mag.*, vol. 42, no. 9, pp. 80–89, 2004.

[2] F. H. Fitzek and M. D. M. D. Katz, *Cooperation in Wireless Networks: Principles and Applications*. Dordrecht, Netherlands: Springer, 2007.

[3] A. Sendonaris, E. Erkip, and B. Aazhang, "User cooperation diversity – parts I & II," *IEEE Trans. Commun.*, vol. 51, no. 11, pp. 1927–1948, 2003.

[4] J. N. Laneman, D. N. C. Tse, and G. W. Wornell, "Cooperative diversity in wireless networks: Efficient protocols and outage behavior," *IEEE Trans. Inf. Theory*, vol. 50, no. 12, pp. 3062–3080, 2004.

[5] A. Wiewiorka and P. N. Moss, "Digital on-channel repeater for DAB," *BBC R&D white paper*, no. WHP120, 2005.

[6] K. Shibuya, "Broadcast-wave relay technology for digital terrestrial television broadcasting," *Proc. IEEE*, vol. 94, no. 1, pp. 269–273, 2006.

[7] T. Maeyama and T. Inoue, "Development of cellular repeater system with radio echo supresser," in *Proc. IEEE Int. Symp. Pers., Indoor and Mobile Radio Comm.*, vol. 4, 2004, pp. 2323–2327.

[8] H. Ju, E. Oh, and D. Hong, "Improving efficiency of resource usage in two-hop full duplex relay systems based on resource sharing and interference cancellation," *IEEE Trans. Wireless Commun.*, vol. 8, no. 8, pp. 3933–3938, 2009.

[9] T. Riihonen, S. Werner, and R. Wichman, "Spatial loop interference suppression in full-duplex MIMO relays," in *Proc. Asilomar Conf. Signals, Syst., Comput.*, 2009, pp. 1508–1512.

[10] S. Mahboob, S. Stapleton, and S. Muhaidat, "Adaptive interference cancellation system for a WCDMA repeater," in *Proc. IEEE Veh. Technol. Conf.-Fall*, 2010.

[11] P. Lioliou, M. Viberg, M. Coldrey, and F. Athley, "Self-interference suppression in full-duplex MIMO relays," in *Proc. Asilomar Conf. Signals, Syst., Comput.*, 2010, pp. 658–662.

[12] S. Berger, M. Kuhn, A. Wittneben, T. Unger, and A. Klein, "Recent advances in amplify-and-forward two-hop relaying," *IEEE Commun. Mag.*, vol. 47, no. 7, pp. 50–56, 2009.

[13] J. R. Treichler, C. R. Johnson Jr., and M. G. Larimore, *Theory and design of adaptive filters*. Upper Saddle River, NJ: Prentice Hall, 2001.

[14] S. Haykin, *Adaptive filter theory*, 3rd ed. Upper Saddle River, NJ: Prentice Hall, 1996.

[15] H. Sakai, T. Oka, and K. Hayashi, "A simple adaptive filter method for cancellation of coupling wave in OFDM signals at SFN relay station," in *Proc. European Signal Process. Conf.*, 2006.

[16] Y.-J. Lee, H. M. Eum, Y.-T. Lee, K. S. Son, and H.-N. Kim, "Performance of feedback cancellers for T-DMB on-channel repeaters," *IEEE Trans. Broadcast.*, vol. 55, no. 4, pp. 810–817, 2009.

[17] K. M. Nasr, J. P. Cosmas, M. Bard, and J. Gledhill, "Performance of an echo canceller and channel estimator for on-channel repeaters in DVB-T/H networks," *IEEE Trans. Broadcast.*, vol. 53, no. 3, pp. 609–618, 2007.

[18] M. Mazzotti, F. Zabini, D. Dardari, and O. Andrisano, "Performance of an echo canceller based on pseudo-noise training sequences," in *Proc. IEEE Broadcast Symp.*, 2008.

[19] Y.-J. Lee, J.-B. Lee, S. I. Park, Y.-T. Lee, H. M. Kim, and H.-N. Kim, "Feedback cancellation for T-DMB repeaters based on frequency-domain channel estimation," *IEEE Trans. Broadcast.*, vol. 57, no. 1, pp. 114–120, 2011.

[20] Y.-T. Lee, S. I. Park, H. M. Eum, J. H. Seo, H. M. Kim, S. W. Kim, and J. S. Seo, "A design of equalization digital on-channel repeater for single frequency network ATSC system," *IEEE Trans. Broadcast.*, vol. 53, no. 1, pp. 23–37, 2007.

[21] S. I. Park, S. R. Park, H. Eum, J.-Y. Lee, Y.-T. Lee, and H. M. Kim, "Equalization on-channel repeater for terrestrial digital multimedia broadcasting system," *IEEE Trans. Broadcast.*, vol. 54, no. 4, pp. 752–760, 2008.

[22] J. Y. Choi, M.-S. Hur, Y.-W. Suh, J.-S. Baek, Y.-T. Lee, and J.-S. Seo, "Interference cancellation techniques for digital on-channel repeaters in T-DMB system," *IEEE Trans. Broadcast.*, vol. 57, no. 1, pp. 46–56, 2011.

[23] R. López-Valcarce, C. Mosquera, F. Pérez-González, and A. Prieto-Davila, "Signal processing system for spectrum shaping," European Patent EP1 744 455 (A2), Jan 17, 2007.

[24] T. Schenk, *RF imperfections in high-rate wireless systems*. Dordrecht, Netherlands: Springer, 2008.

[25] K. J. Åström and T. S. Söderström, "Uniqueness of the maximum likelihood estimates of the parameters of an ARMA model," *IEEE Trans. Autom. Control*, vol. 19, no. 6, pp. 769–773, 1974.

[26] P. A. Regalia, *Adaptive IIR Filtering in Signal Processing and Control*. New York: Marcel Dekker, 1994.

[27] P. L. Feintuch, "An adaptive recursive LMS filter," *Proc. IEEE*, vol. 64, no. 11, pp. 1622–1624, 1976.

[28] EN 300 744 V1.5.1, *Digital Video Broadcasting (DVB); Framing structure, channel coding and modulation for terrestrial television*. ETSI, Nov. 2004.

[29] D. Fasino, "Spectral properties of Toeplitz-plus-Hankel matrices," *Calcolo*, vol. 33, no. 1–2, pp. 87–98, 1996.